

An *Slfn2* mutation causes lymphoid and myeloid immunodeficiency due to loss of immune cell quiescence

Michael Berger¹, Philippe Krebs¹, Karine Crozat^{1,4}, Xiaohong Li¹, Ben A Croker^{1,4}, Owen M Siggs¹, Daniel Popkin², Xin Du¹, Brian R Lawson², Argyrios N Theofilopoulos², Yu Xia¹, Kevin Khovananth¹, Eva Marie Y Moresco¹, Takashi Satoh³, Osamu Takeuchi³, Shizuo Akira³ & Bruce Beutler¹

Here we describe a previously unknown form of inherited immunodeficiency revealed by an *N*-ethyl-*N*-nitrosourea-induced mutation called *elektra*. Mice homozygous for this mutation showed enhanced susceptibility to bacterial and viral infection and diminished numbers of T cells and inflammatory monocytes that failed to proliferate after infection and died via the intrinsic apoptotic pathway in response to diverse proliferative stimuli. They also had a greater proportion of T cells poised to replicate DNA, and their T cells expressed a subset of activation markers, suggestive of a semi-activated state. We positionally ascribe the *elektra* phenotype to a mutation in the gene encoding Schlafen-2 (*Slfn2*). Our findings identify a physiological role for *Slfn2* in the defense against pathogens through the regulation of quiescence in T cells and monocytes.

The immune system maintains a vast repertoire of B cells and T cells waiting to respond to microbial invasion. These quiescent, naive lymphocytes may be activated by antigen engagement and costimulation, triggering an exit from the G0 phase of the cell cycle, entry into active cell cycle and higher metabolism as cells both expand their populations and acquire effector functions. Published studies have demonstrated that lymphocyte quiescence, a state of reversible growth arrest in which cells remain responsive to activating stimuli and resistant to apoptosis (and are therefore not anergic), must be actively maintained by the action of molecules that include transcription factors and cell-cycle regulators¹. DNA microarray experiments suggest that specific transcriptional programs are associated with the quiescent state^{2,3} and that cellular activation involves not only increased expression of genes that promote growth and differentiation but also suppression of a quiescent gene-expression program^{4,5}. A growing number of known genes, including *Foxo1*, *Foxo2*, *Foxo3* (ref. 6), *Klf2* (ref. 7) and *Tob8*⁸, have been linked to the regulation of the quiescence of cells of the immune response.

Here we describe an inherited immune deficiency characterized by susceptibility to both bacterial and viral infections, in which thymocytes developed normally but peripheral T cells died in response to activating or homeostatic expansion stimuli. Activation also triggered death of inflammatory monocytes. The majority of peripheral T cells had a semiactivated phenotype, and this population of cells specifically underwent apoptosis through the intrinsic apoptotic pathway. We positionally ascribed the cause of this immune deficiency to a

mutation (*elektra*) in *Slfn2*, which demonstrates a role for *Slfn2* in maintaining quiescence in cells of the immune response *in vivo*.

RESULTS

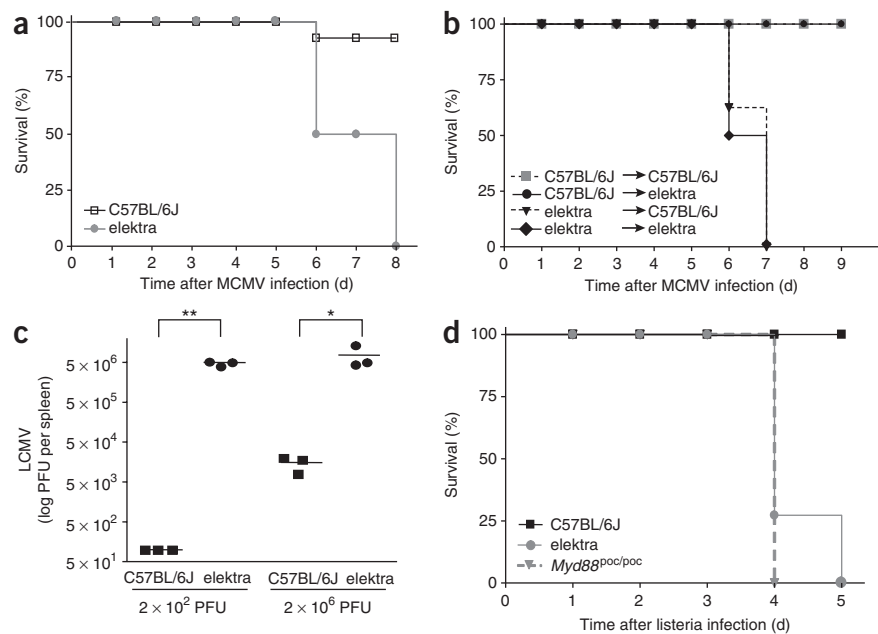
Immunodeficiency of *elektra*-mutant mice

We detected the recessive *elektra* phenotype among G₃ mice homozygous for random germline mutations induced by *N*-ethyl-*N*-nitrosourea. We screened mice for mutations that caused a lethal outcome after mice were inoculated with normally sublethal quantities of mouse cytomegalovirus (MCMV)⁹. Mice homozygous for the *elektra* mutation died 6–8 d after being inoculated with 2×10^5 plaque-forming units (PFU) of MCMV, whereas nearly all C57BL/6J wild-type control mice survived (Fig. 1a). Serum cytokine concentrations in *elektra* homozygotes were similar to those in wild-type mice for this infection model (Supplementary Fig. 1a), which suggested that this mutation did not confer an innate immune sensing defect. Moreover, the *elektra* mutation did not impair natural killer (NK) cell function, which is critical for controlling MCMV infection¹⁰, as killing of NK target cells and production of interferon- γ (IFN- γ) after activation of NK cells was intact (Supplementary Fig. 1b,c). The susceptibility phenotype was completely 'rescued' by transplantation of bone marrow from wild-type mice (Fig. 1b), which suggested that a hematopoietic defect was responsible for this phenotype. Further characterization demonstrated that the immune defect in *elektra* homozygotes was not restricted to the containment of MCMV infection. Lymphocytic choriomeningitis virus (LCMV; Armstrong

¹Department of Genetics and ²Department of Immunology and Microbial Sciences, The Scripps Research Institute, La Jolla, California, USA. ³Department of Host Defense, Research Institute for Microbial Diseases, Osaka University, Osaka, Japan. ⁴Present addresses: Centre d'Immunologie de Marseille-Luminy, Marseille, France (K.C.) and Cancer and Haematology Division, The Walter and Eliza Hall Institute of Medical Research, Parkville, Australia (B.A.C.). Correspondence should be addressed to B.B. (bruce@scripps.edu).

Received 12 November 2009; accepted 25 January 2010; published online 28 February 2010; doi:10.1038/ni.1847

Figure 1 Mice homozygous for the *elektra* mutation are highly susceptible to infection with MCMV, LCMV and *L. monocytogenes*. (a) Survival curves for wild-type mice ($n = 8$) and *elektra* homozygotes ($n = 8$) after challenge with 2×10^5 PFU of MCMV. (b) Survival curves after infection with 2×10^5 PFU of MCMV, assessed in recipient mice reconstituted with 5×10^6 bone marrow cells (reciprocal bone marrow transplantation) 1 d after a 10-Gy dose of irradiation (C57BL/6J→C57BL/6J, $n = 3$; C57BL/6J→*elektra*, $n = 6$; *elektra*→C57BL/6J, $n = 6$; *elektra*→*elektra*, $n = 3$; congenic C57BL/6.SJL (*Ptprc^aPep3^b*; Ly5.1⁺), C57BL/6J (*Ptprc^bPep3^b*; Ly5.2⁺) wild-type and *elektra* mutant mice serve as both recipients and donors). (c) Viral load in spleens of wild-type and *elektra* homozygotes ($n = 3$ mice per group) 7 d after intravenous injection of 2×10^2 or 2×10^6 PFU of LCMV (Armstrong strain). Each symbol represents an individual mouse; small horizontal lines indicate the mean. * $P = 0.028$ and ** $P < 0.0001$ (two-tailed Student's *t*-test). (d) Survival curves for wild-type mice ($n = 5$), *elektra* homozygotes ($n = 7$) and mice deficient in Toll-like receptor signaling due to mutation of *Myd88* (*Myd88^{poc/poc}*; $n = 2$) challenged with 2×10^5 colony-forming units of *L. monocytogenes*. Results are representative of five (a), two (b,c) or four (d) independent experiments.



strain) proliferated excessively in *elektra* homozygotes, whereas it was effectively cleared from wild-type mice by 7 d after infection (Fig. 1c). Moreover, *elektra* homozygotes died 4–5 d after intravenous injection with *Listeria monocytogenes* because of an impaired ability to control bacterial growth. The magnitude of susceptibility was similar to that observed in mice deficient in Toll-like receptor signaling due to mutation of *Myd88*, which encodes a critical Toll-like receptor adaptor protein¹¹ (Fig. 1d and Supplementary Fig. 1d). Thus, despite having normal innate sensing, *elektra* homozygotes show susceptibility to diverse infections, which stems from a defect in the hematopoietic compartment.

A defect in peripheral T cells

To characterize the immunological defect caused by the *elektra* mutation, we immunophenotyped cells by flow cytometry. Mice homozygous for the *elektra* mutation had normal cellularity of the spleen, thymus,

lymph nodes and peripheral blood. Low percentages of CD4⁺ and CD8⁺ T cells were evident both in the spleen and lymph nodes relative to those of wild-type mice. The percentage of CD8⁺ T cells was much lower in blood, whereas the percentage of CD4⁺ T cells was slightly lower (Fig. 2a). However, thymic T cell populations were normal, as assessed by the ratios of double-negative (CD4⁻CD8⁻) cells, double-positive (CD4⁺CD8⁺) cells and single-positive cells, as well as total thymocyte numbers (Fig. 2b and data not shown). Control of LCMV infection is dependent on CD8⁺ T cell activity, and infection of wild-type mice with LCMV (Armstrong strain) leads to a sharp increase in CD8⁺ T cell numbers. Consistent with their failure to restrict the proliferation of LCMV (Fig. 1c), *elektra* homozygotes had fewer CD8⁺ T cells after LCMV infection (Fig. 2c, top). Moreover, restimulation of splenocytes from LCMV-infected *elektra* homozygotes *ex vivo* with LCMV-derived peptides (representing immunodominant epitopes of both envelope and nuclear protein antigens) resulted in considerably fewer IFN- γ -producing CD8⁺ cells than wild-type mice had (Fig. 2c, bottom). These findings demonstrate that the *elektra* mutation impaired both the number and the response of T cells.

Activation signals lead to T cell death

To understand the peripheral T cell deficiency observed in *elektra* homozygotes, we first stimulated lymph node-derived lymphocytes

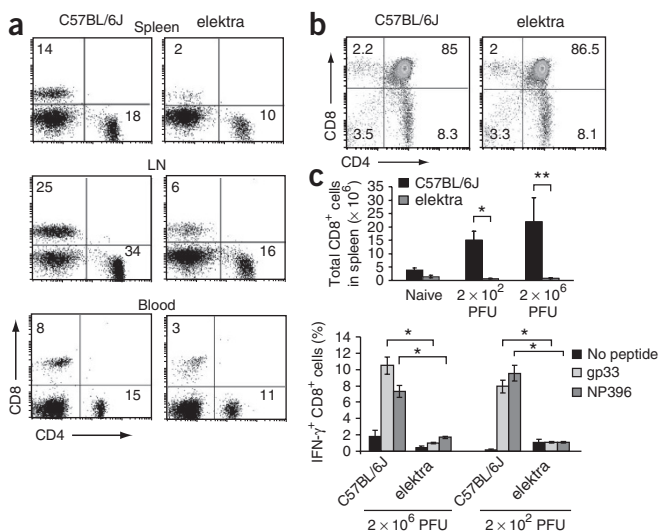


Figure 2 Defect in peripheral T cells in *elektra* homozygotes. (a,b) Flow cytometry analysis of the expression of CD4 and CD8 by cells from the spleen, lymph node (LN) and blood (a) or by thymocytes (b) from wild-type or *elektra*-homozygous mice. Numbers in quadrants indicate percent cells in each. (c) Total CD8⁺ splenocytes among splenocytes isolated from wild-type and *elektra*-homozygous mice 7 d after intravenous injection of 2×10^2 or 2×10^6 PFU of LCMV, Armstrong strain (top), and frequency of cells with intracellular IFN- γ expression among CD8⁺ splenocytes then restimulated *ex vivo* with gp33 or NP396 (peptides derived from LCMV) in the presence of brefeldin A (bottom). * $P < 0.01$ and ** $P < 0.001$ (two-tailed Student's *t*-test). Results are representative of three experiments with ten mice per genotype (a,b) or two independent experiments with three mice per genotype per condition (c; error bars, s.d.).

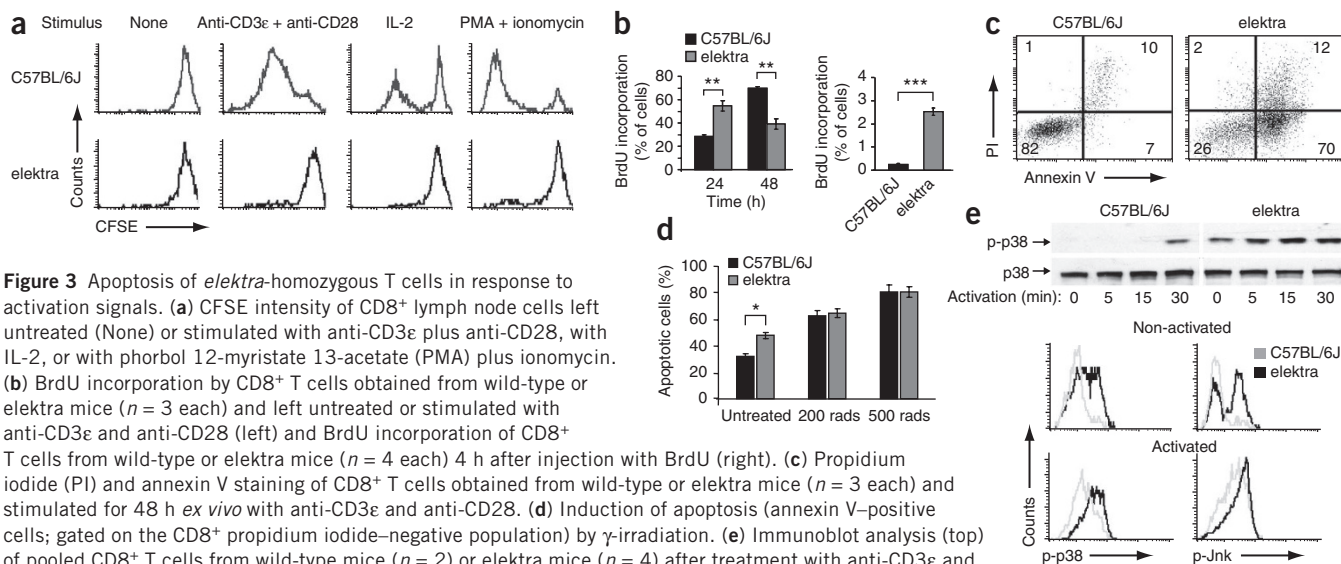


Figure 3 Apoptosis of *elektra*-homozygous T cells in response to activation signals. **(a)** CFSE intensity of CD8⁺ lymph node cells left untreated (None) or stimulated with anti-CD3ε plus anti-CD28, with IL-2, or with phorbol 12-myristate 13-acetate (PMA) plus ionomycin. **(b)** BrdU incorporation by CD8⁺ T cells obtained from wild-type or *elektra* mice ($n = 3$ each) and left untreated or stimulated with anti-CD3ε and anti-CD28 (left) and BrdU incorporation of CD8⁺ T cells from wild-type or *elektra* mice ($n = 4$ each) 4 h after injection with BrdU (right). **(c)** Propidium iodide (PI) and annexin V staining of CD8⁺ T cells obtained from wild-type or *elektra* mice ($n = 3$ each) and stimulated for 48 h *ex vivo* with anti-CD3ε and anti-CD28. **(d)** Induction of apoptosis (annexin V-positive cells; gated on the CD8⁺ propidium iodide-negative population) by γ -irradiation. **(e)** Immunoblot analysis (top) of pooled CD8⁺ T cells from wild-type mice ($n = 2$) or *elektra* mice ($n = 4$) after treatment with anti-CD3ε and anti-CD28, assessed with antibody to phosphorylated p38 (p-p38) or anti-p38 and flow cytometry analysis (bottom) of the staining of phosphorylated p38 (p-p38) or phosphorylated Jnk (p-Jnk) in wild-type ($n = 3$) or *elektra* ($n = 3$) CD8⁺ T cells. * $P < 0.05$, ** $P < 0.01$ and *** $P < 0.001$ (two-tailed Student's *t*-test). Results are representative of four experiments with three mice per genotype (a), two experiments (b,c), two experiments with three mice per genotype (d) or three experiments (e). Error bars (b,d), s.d.

for 72 h *in vitro* with a combination of antibody to CD3ε (anti-CD3ε) and anti-CD28, with interleukin 2 (IL-2), or with a combination of phorbol 12-myristate 13-acetate and ionomycin. Both CD8⁺ T cells and CD4⁺ T cells (data not shown) from *elektra* homozygotes failed to expand their populations normally in response to these stimuli (Fig. 3a). Further examination of the proliferative response to activation of the T cell antigen receptor (TCR) with an *in vitro* bromo-2-deoxyuridine (BrdU)-incorporation assay demonstrated that in fact a higher percentage of *elektra*-homozygous CD8⁺ T cells than wild-type cells incorporated BrdU after stimulation for 24 h with anti-CD3ε plus anti-CD28 (Fig. 3b, left), which indicated that *elektra*-homozygous T cell populations are not growth arrested and even contain a greater proportion of activation-competent cells. However, we obtained the opposite result after 48 h of activation, when fewer *elektra*-homozygous CD8⁺ T cells than wild-type cells replicated DNA (Fig. 3b, left). Consistent with those results, a greater percentage of mutant CD8⁺ T cells incorporated BrdU *in vivo* under steady-state conditions (Fig. 3b, right). Annexin V staining at 48 h after activation showed massive apoptosis of mutant CD8⁺ T cells (Fig. 3c). However, γ -irradiation-induced apoptosis was equivalent in *elektra*-homozygous and wild-type CD8⁺ T cells (Fig. 3d), which indicated that the *elektra* mutation selectively causes death in response to activation.

Signals from the TCR control the activity of several pathways, including those of the transcription factors NF- κ B and NFAT and the mitogen-activated protein kinases Akt, Erk1/2, Jnk and p38, which together determine whether T cells will survive and proliferate or die through apoptosis^{12–16}. We examined the activation status of each pathway in the first hour after TCR stimulation of wild-type or *elektra*-homozygous CD8⁺ T cells with beads coated with anti-CD3ε and anti-CD28. In *elektra*-homozygous cells, we found normal TCR-stimulated calcium influx (Supplementary Fig. 2a), dephosphorylation of NFAT (Supplementary Fig. 2b), nuclear translocation of NF- κ B (Supplementary Fig. 2c) and phosphorylation of Erk and Akt (Supplementary Fig. 2d,e), which demonstrated intact signaling through these T cell activation and survival pathways during the initial response to TCR stimulation. T cells from *elektra* homozygotes also

showed normal induction of the activation markers CD25 and CD69 at 24 h after TCR activation (Supplementary Fig. 2f). However, p38 and Jnk, which are activated through phosphorylation, were constitutively phosphorylated under basal conditions and were further phosphorylated after TCR stimulation in *elektra*-homozygous CD8⁺ T cells (Fig. 3e).

Collectively, the data reported above demonstrated that compared with wild-type cells, *elektra*-homozygous CD8⁺ T cells initiated responses to TCR activation normally, with a greater proportion of cells replicating DNA after 24 h of activation. By 48 h, most *elektra* cells had become apoptotic. These results suggest that the *elektra* phenotype entails both hypersensitivity to an activating stimulus and fragility after activation.

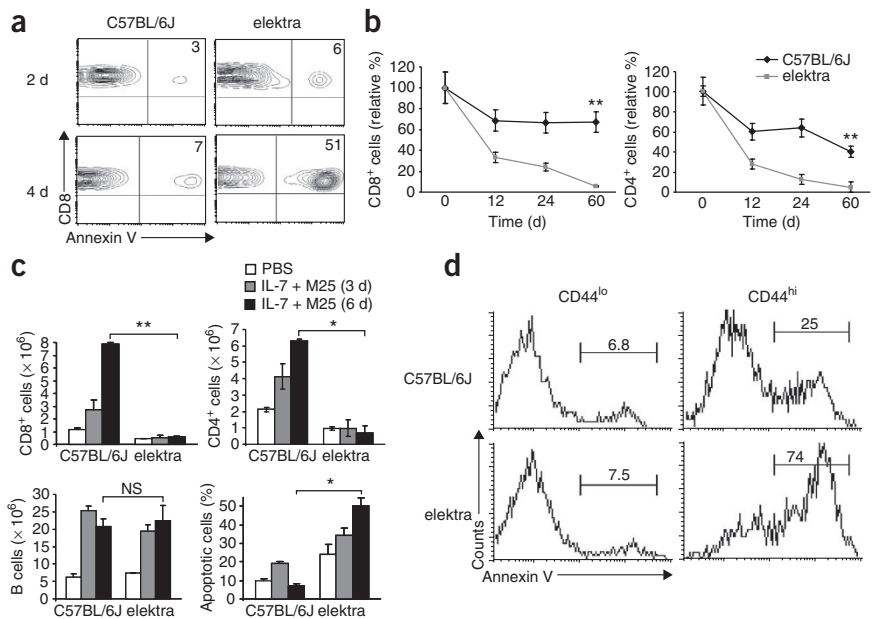
Death of *elektra* T cells in response to expansion signals

To further test the proliferative capacity of *elektra*-homozygous T cells, we examined their response to homeostatic proliferation signals. We labeled wild-type and *elektra*-homozygous (Ly5.2⁺) splenocytes with the cytosolic dye CFSE and adoptively transferred them into sublethally irradiated wild-type (Ly5.1⁺) recipients. Wild-type T cells underwent proliferation as expected, but we detected no *elektra*-homozygous T cells in the spleen 7 d after infusion (Supplementary Fig. 3a). When we collected spleens 2 and 4 d after adoptive transfer, we found that an excess of the *elektra*-homozygous mutant cells were apoptotic, as indicated by annexin V staining (Fig. 4a). B cells homozygous for the *elektra* mutation were present in percentages similar to those of wild-type B cells in recipient mice (Supplementary Fig. 3b). To monitor the fate of existing peripheral T cells, we blocked their replenishment with new thymic emigrants by thymectomy of adult mice. Wild-type T cell numbers decreased by 30% after thymectomy and then remained stable for more than 60 d. In contrast, *elektra*-homozygous T cells decreased considerably within 12 d of thymectomy and almost completely disappeared from the blood by 60 d after thymectomy (Fig. 4b).

We also tested homeostatic population expansion of T cells in response to injection of IL-7 together with non-neutralizing anti-IL-7. This treatment mimics the lymphopenic condition and results

Figure 4 Apoptosis of *elektra*-homozygous T cells in response to homeostatic expansion signals.

(a) Annexin V staining of adoptively transferred wild-type or *elektra* CD8⁺CD45.1⁻ cells from spleens of wild-type (Ly5.1⁺) recipient mice ($n = 4$). Numbers in top right quadrants indicate percent CD8⁺ apoptotic cells. (b) CD8⁺ T cells (left) and CD4⁺ T cells (right) in 7-week-old wild-type or *elektra* mice ($n = 5$ or 6, respectively) at various times after thymectomy, presented as relative percent of T cells ((% T cells in blood after thymectomy) / (% T cells in blood before thymectomy) × 100). (c) Number of CD8⁺ T cells, CD4⁺ T cells and B cells and frequency of annexin V-positive (apoptotic) CD8⁺ T cells, in spleens from wild-type or *elektra* mice ($n = 4$ each) injected with PBS (white) or with IL-7 plus anti-IL-7 (M25) on days 1 and 3, with cells collected on day 6 (black), or on day 1, with cells collected on day 3 (gray). (d) Annexin V staining of splenic CD8⁺CD44^{hi} or CD8⁺CD44^{lo} cells from wild-type or *elektra* mice ($n = 4$ each). Numbers above bracketed lines indicate percent apoptotic cells. NS, not significant; * $P < 0.01$ and ** $P < 0.001$ (two-tailed Student's *t*-test). Results are representative of three (a,d) or two (b,c) experiments. Error bars (b,c), s.d.



in the population expansion of both T cells and B cells¹⁷. As expected, in contrast to injection with PBS, injection of IL-7 plus anti-IL-7 resulted in the population expansion of both B cells and T cells, as well as a lower percentage of annexin V-positive CD8⁺ T cells after 6 d, in wild-type mice (Fig. 4c). Whereas B cell populations expanded normally in *elektra* homozygotes, both CD8⁺ and CD4⁺ T cells failed to proliferate in response to treatment with IL-7 plus anti-IL-7 (Fig. 4c). Moreover, in contrast to cells from wild-type mice, a higher percentage of CD8⁺ T cells from *elektra*-homozygous mice were positive for annexin V 6 d after treatment with IL-7 plus anti-IL-7 than after PBS injection (Fig. 4c, bottom), which suggested that they die in response to signals induced by IL-7.

The cell surface glycoprotein CD44 normally accumulates on T cells as they mature in the periphery: naive T cells that have newly emigrated from the thymus have low expression of CD44, whereas mature, expanding T cell populations have abundant expression of CD44. *In vitro*, experimental signals for homeostatic population expansion also induce CD44 surface expression^{18–20}. We examined the annexin V staining of CD44^{hi} and CD44^{lo} populations of splenic CD8⁺ T cells from *elektra*-homozygous and wild-type mice under steady-state conditions. Regardless of genotype, most of the annexin V-positive cells were CD44^{hi}. Although similar small percentages of wild-type and mutant CD44^{lo} cells were annexin V positive, the percentage of annexin V-positive CD44^{hi} *elektra*-homozygous cells was much greater than that of wild-type cells (Fig. 4d). Together these findings demonstrate that *elektra*-homozygous CD44^{hi} CD8⁺ T cells die in response to homeostatic expansion signals.

T cells die via the intrinsic apoptotic pathway

Homeostatic lymphoid cell death is required for the elimination of cells that are no longer needed once an infection is resolved and for the elimination of potentially autoreactive cells. It is mediated both by the intrinsic apoptotic signaling pathway (controlled by the balance of pro- and antiapoptotic Bcl-2 family members) and the extrinsic apoptotic signaling pathway (controlled by signals from receptors for tumor necrosis factor, the CD95 ligand and the proapoptotic molecule TRAIL). We examined the status of both pathways

in *elektra*-homozygous mice. We excluded the Fas-mediated extrinsic pathway as the mechanism of cell death in *elektra*-homozygous T cells because we observed no restoration of CD8⁺ or CD4⁺ T cells in double-mutant mice homozygous for both the *elektra* mutation and the lymphoproliferation mutation of *Fas* (Fig. 5a).

The intrinsic pathway is chiefly responsible for T cell death after clonal expansion induced by acute, time-limited TCR activation that occurs during infection or homeostatic expansion^{21–23}. The antiapoptotic protein Bcl-2, which sequesters proapoptotic Bim and prevents activation of the other proapoptotic proteins Bax and Bak, is a key regulator of apoptosis mediated by the intrinsic pathway²⁴. Consistent with the finding that apoptosis of *elektra*-homozygous T cells was greater in the CD44^{hi} population (Fig. 4d), Bcl-2 expression was specifically lower in the CD44^{hi} population (Fig. 5b). Notably, the death of CD4⁺ and CD8⁺ T cells was completely 'rescued' in *elektra*-homozygous mice expressing a *BCL2* transgene (Fig. 5c). Moreover, the *BCL2* transgene partially restored the ability of *elektra*-homozygous CD4⁺ T cells (data not shown) and CD8⁺ T cells (Fig. 5d) to proliferate *in vitro* in response to TCR stimulation. These results demonstrate that the death of *elektra*-homozygous T cells is mediated by the intrinsic apoptotic pathway through the action of Bcl-2 family members and that T cells from *elektra* homozygotes are able to proliferate once their propensity for apoptosis is blocked.

T cells exist in a semiactivated state

The CD44^{hi} population encompasses both recently activated and memory-phenotype cells, which may be discriminated on the basis of expression of the IL-2 receptor β -chain (IL-2R β (CD122)), which is higher in cells with a memory phenotype²⁵. In wild-type spleens, the CD44^{hi} CD8⁺ T cell population was composed mostly of CD122⁺ cells, but in *elektra*-homozygous spleens, most of the CD44^{hi} CD8⁺ and CD4⁺ T cells were CD122⁻ (Fig. 6a, left, and Supplementary Fig. 4a, respectively). Induction of homeostatic T cell population expansion in *elektra* homozygotes by injection of an IL-7-anti-IL-7 complex resulted in a higher percentage of cells with this altered CD122 expression (Fig. 6a, right). This CD44^{hi}CD122⁻ population showed complete shedding of the lymph node-homing

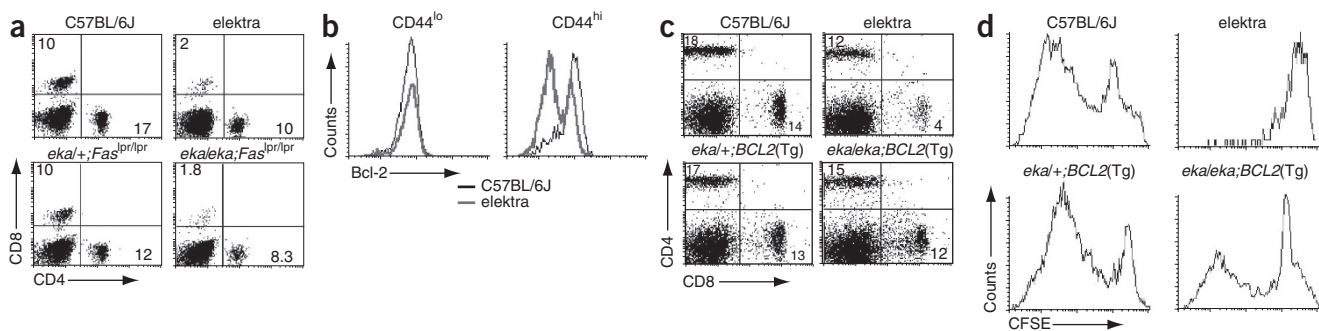


Figure 5 T cells homozygous for the *elektra* mutation die via the intrinsic apoptotic pathway. (a) Staining of CD4 and CD8 in blood cells from 6-week-old littermate offspring of crosses of mice homozygous for the *elektra* mutation (*eka*) with mice homozygous for the lymphoproliferation mutation (*lpr*) of *Fas* to generate double-mutant mice (*ekaleka; Fas^{lpr/lpr}*). Numbers in quadrants indicate percent CD8⁺CD4⁻ cells (top left) or CD8⁻CD4⁺ cells (bottom right). (b) Flow cytometry of Bcl-2 expression in splenic CD8⁺CD44^{hi} or CD8⁺CD44^{lo} cells from wild-type or *elektra*-homozygous mice. (c) Staining of CD4 and CD8 on splenic cells from 4-week-old littermate offspring from crosses of *ekaleka* and *eka+* mice expressing a *BCL2* transgene (*BCL2(Tg)*) to generate *elektra* homozygotes overexpressing Bcl-2 in T cells. Numbers in quadrants indicate percent CD4⁺CD8⁻ cells (top left) or CD4⁻CD8⁺ cells (bottom right). (d) Flow cytometry of the CFSE intensity of CD3⁺CD8⁺ cells among CFSE-labeled spleen cells from the mice in c, stimulated *in vitro* with a combination of anti-CD3ε and anti-CD28 and collected after 72 h. Results are representative of two independent experiments with three to four mice per genotype in each.

receptor CD62L (L-selectin), no expression of the IL-7 receptor α -chain (IL-7R α (CD127)) and low CD5 expression (Fig. 6b, right), which suggested that these cells were recently activated. In addition, the CD44^{lo} (naive) population of CD8⁺ and CD4⁺ T cells in *elektra* homozygotes had low expression of both IL-7R α and CD62L (Fig. 6b,

left, and Supplementary Fig. 4b). Low expression of CD62L, in contrast to complete shedding of the CD62L molecule, has been shown to occur in response to continuous TCR stimulation^{26,27}. Similarly, low expression of IL-7R α is associated with T cell activation. However, *elektra*-homozygous CD8⁺ T cells (both CD44^{hi} and CD44^{lo}) had

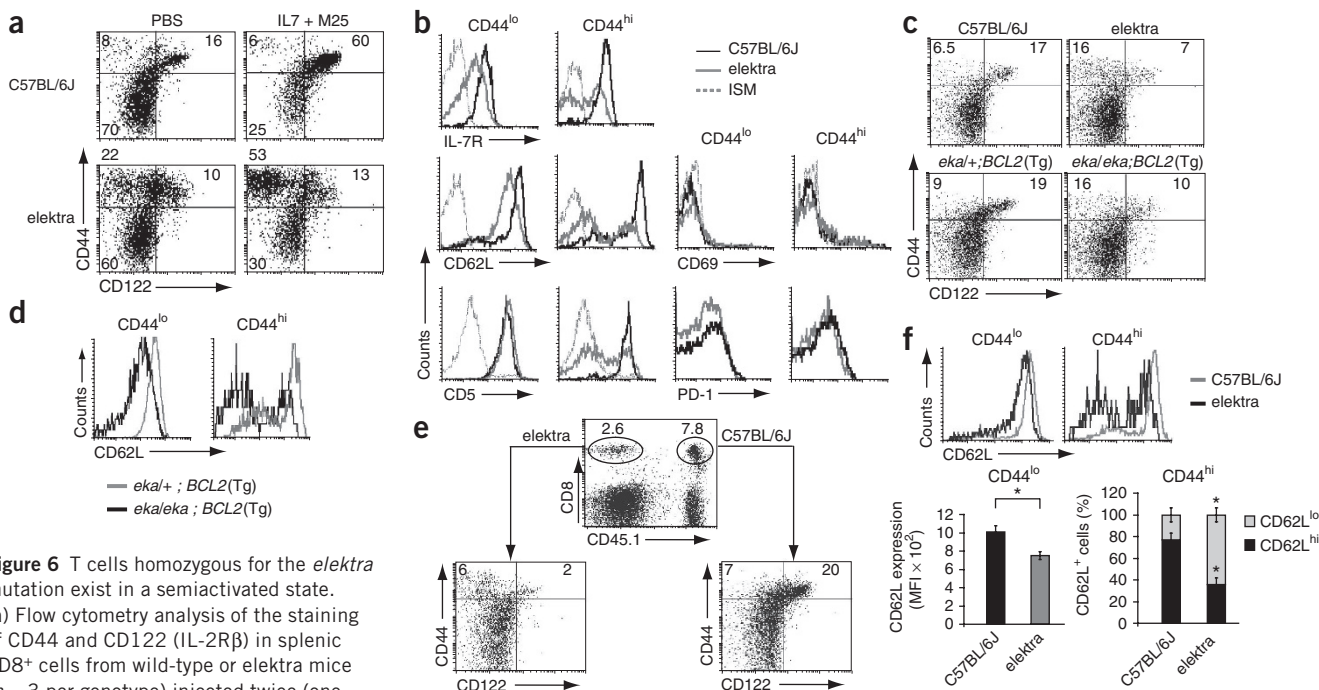


Figure 6 T cells homozygous for the *elektra* mutation exist in a semiactivated state.

(a) Flow cytometry analysis of the staining of CD44 and CD122 (IL-2R β) in splenic CD8⁺ cells from wild-type or *elektra* mice ($n = 3$ per genotype) injected twice (one dose every 3 d) with PBS or with IL-7 plus anti-IL-7. Numbers in quadrants indicate percent cells in each. (b) Flow cytometry of CD44^{lo}CD8⁺ or CD44^{hi}CD8⁺ cells stained for IL-7R α , CD62L, CD5, CD69 or PD-1 ($n = 3$ mice per genotype). ISM, isotype-matched control antibody. (c) Staining of CD44 and CD122 in splenic CD8⁺ cells from 4-week-old littermates of various genotypes (above plots; $n = 3$ mice per genotype). Numbers in quadrants indicate percent CD44^{hi}CD122⁻ cells (top left) or CD44^{hi}CD122⁺ cells (top right). (d) CD62L staining of spleen CD44^{lo}CD8⁺ or CD44^{hi}CD8⁺ cells from *elektra*-heterozygous mice (*ekaleka*) or *elektra*-homozygous mice (*ekaleka*) expressing a *BCL2* transgene ($n = 3$ per genotype). (e, f) Flow cytometry of wild-type (CD45.1⁺) and *elektra* (CD45.2⁺) donor CD8⁺ T cells in CD3-deficient mixed-bone marrow chimeras. (e) CD44 versus CD122 staining. (f) CD62L staining of CD44^{lo}CD8⁺ or CD44^{hi}CD8⁺ cells (top). Below, mean fluorescence intensity (MFI) of CD62L staining in the CD44^{lo} population (left) and frequency of CD62L^{hi} and CD62L^{lo} cells in the CD44^{hi} population (right). * $P < 0.001$ (two-tailed Student's *t*-test). Results are representative of two (a, c, d) or three (b) experiments or two experiments with six recipient mice (e, f). Error bars, s.d.

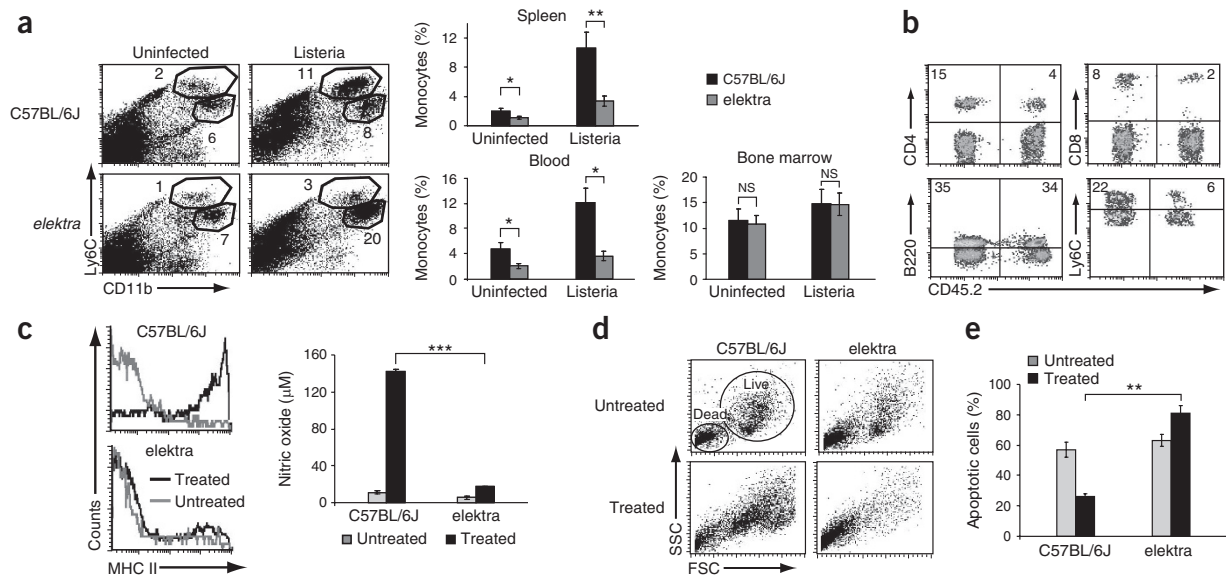


Figure 7 Apoptosis of *elektra*-homozygous monocytes in response to activation signals. **(a)** Ly6C and CD11b staining (left) of splenocytes from uninfected or *L. monocytogenes*-infected wild-type or *elektra* mice ($n = 5$ per genotype). Numbers adjacent to outlined areas indicate percent inflammatory monocytes (R1 gate; top left) or neutrophils (R2 gate; bottom right). Right, frequency of inflammatory monocytes from spleen, blood and bone marrow of wild-type or *elektra* mice ($n = 5$ each) without infection or at 48 h after infection. **(b)** Flow cytometry of wild-type (CD45.2⁻) and *elektra* (CD45.2⁺) donor CD4⁺ T cells, CD8⁺ T cells, B cells (B220⁺) and inflammatory monocytes (gated on CD11b⁺ population) in the blood of CD3-deficient mixed-bone marrow chimeras ($n = 3$). Numbers in quadrants indicate percent cells in each. **(c–e)** Analysis of isolated bone marrow inflammatory monocytes from wild-type or *elektra* mice ($n = 2$ each) cultured for 3 d in medium alone (Untreated) or in medium supplemented with IFN- γ and heat-killed *L. monocytogenes* (Treated). **(c)** MHC class II staining (left) and nitric oxide concentration (right). **(d)** Forward-scatter (FSC) and side-scatter (SSC) profiles. Outlined areas (top left) indicate populations of live and dead cells. **(e)** Annexin V staining of the gated high-forward-scatter population. * $P < 0.05$, ** $P < 0.01$ and *** $P < 0.001$ (two-tailed Student's *t*-test). Results are representative of three **(a,c,e)** or two **(b)** experiments. Error bars **(a,c,e)**, s.d.

normal expression of the activation marker CD69 (Fig. 6b), which suggested that they were not fully activated. CD8⁺ T cells from *elektra* homozygotes were also not exhausted, as indicated by normal expression of the cell survival factor PD-1 (Fig. 6b). These findings suggest that *elektra*-homozygous T cells exist in a partially activated state that predisposes them to apoptosis in response to activation stimuli.

Unexpectedly, although the *BCL2* transgene 'rescued' T cell death in *elektra* homozygotes (Fig. 5c), it did not prevent the development of a semiactivated phenotype by either CD44^{hi} or CD44^{lo} T cells from *elektra* homozygotes (Fig. 6c,d). Moreover, in nonlymphopenic mixed-bone marrow chimeras (lethally irradiated *Cd3* deficient recipients given a mixture (1:1) of *elektra*-homozygous (Ly5.2⁺) cells and wild-type (Ly5.1⁺) cells), *elektra*-homozygous T cells had the same semiactivated phenotype (Fig. 6e,f). This result indicates that the semiactivated state, although exacerbated by lymphopenic conditions (Fig. 4a–c), is not driven primarily by the lymphopenic environment in *elektra* homozygotes. Instead, it is intrinsic to *elektra*-homozygous T cells and apoptosis is a consequence.

Monocytes die in response to activation signals

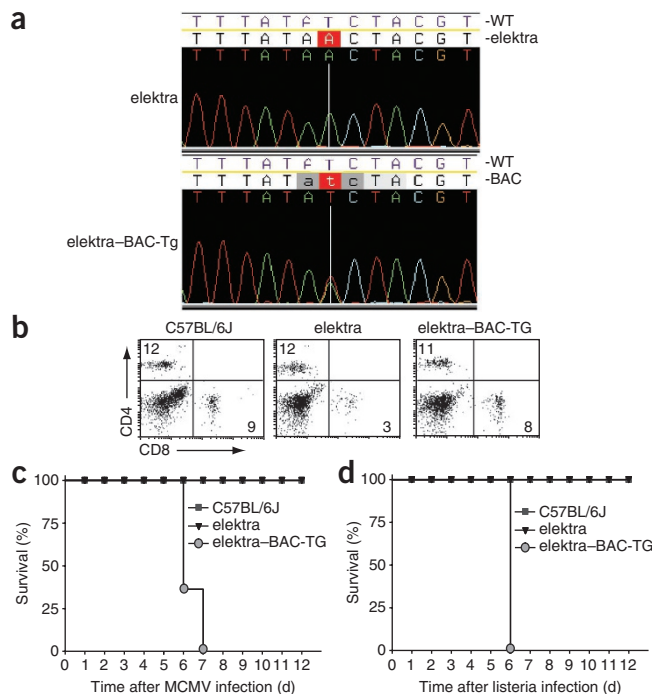
Inflammatory monocyte recruitment is essential for the defense against *L. monocytogenes* in mice²⁸. As *elektra* homozygotes were highly susceptible to *L. monocytogenes*, we examined the inflammatory monocytes in these mice before and during infection. Before infection, *elektra* homozygotes had a normal percentage of inflammatory monocytes in the bone marrow but had a slightly lower percentage of these cells in the blood and spleen than did wild-type mice (Fig. 7a, gated R1 population). After infection, the fraction of inflammatory monocytes increased far less in the blood and spleen

of *elektra* homozygotes than in those of wild-type mice (Fig. 7a). We observed no accumulation of inflammatory monocytes in the bone marrow (Fig. 7a), which indicated that a migration problem did not cause this aspect of the *elektra* phenotype. In contrast to inflammatory monocytes, we found a normal percentage of neutrophils in *elektra* homozygotes under steady-state conditions. We found a higher percentage of neutrophils in *elektra* homozygotes after listeria infection (Fig. 7a, gated R2 population). The exaggerated accumulation of neutrophils after infection may be attributed to the greater bacterial burden in *elektra* homozygotes, as shown before for mice deficient in the CCR2 chemokine receptor²⁸. Macrophage numbers and recruitment to the peritoneal cavity were normal in *elektra* homozygotes, as were macrophage responses to Toll-like receptor ligands *in vitro* (data not shown). Dendritic cells were present in normal numbers (data not shown), and when stimulated with unmethylated CpG oligonucleotides, these cells survived and upregulated the costimulatory molecule CD40 as effectively as wild-type cells did (Supplementary Fig. 5). In mixed-bone marrow chimeras (generated as described above), both T cells and inflammatory monocytes derived from *elektra* homozygotes were disfavored compared with cells of wild-type origin, whereas we observed equal percentages of B cells and neutrophils of *elektra*-homozygous and wild-type origin (Fig. 7b). Together these findings indicate a cell-intrinsic, lineage-specific effect of the *elektra* mutation.

We determined whether the CD11b⁺Ly6C^{hi} monocytes from *elektra* homozygotes were more prone to apoptosis in response to bacterial stimuli. We sorted CD11b⁺Ly6C^{hi}Ly6G⁻ monocytes from the bone marrow of uninfected mice, cultured the cells for 3 d *in vitro* in the presence of IFN- γ and heat-killed *L. monocytogenes*,

Figure 8 'Rescue' of the *elektra* phenotype by BAC transgenesis.

(a) DNA sequence of the BAC clone and genomic DNA from an *Slfn2*^{eka/eka} mouse in the region of the *Slfn2*^{eka} mutation. The BAC clone contains the wild-type *Slfn2* sequence. Gray highlighting indicates that the nucleotide of interest is in heterozygous form in the transgenic mouse (wild-type nucleotide from the BAC transgene; mutated nucleotide from the genomic DNA); red highlighting indicates nucleotides of interest; lower case indicates heterozygosity; curved lines indicate sequencing peaks (colors match nucleotides above). (b) Flow cytometry analysis of the staining of CD8 and CD4 in blood from a wild-type mouse, an *Slfn2*^{eka/eka} mouse carrying the *Slfn2* transgene (*elektra*-BAC-Tg) and a littermate lacking the transgene (*elektra*). Results are representative of three experiments with four mice per genotype. (c) Survival curves for BAC-transgenic mice ($n = 7$), littermates without the BAC transgene ($n = 4$) and wild-type mice ($n = 5$) after challenge with 2×10^5 PFU of MCMV. Results are representative of two experiments. (d) Survival curves for BAC-transgenic mice ($n = 7$), littermates without the BAC transgene ($n = 5$) and wild-type mice ($n = 7$) after challenge with 5×10^5 colony-forming units of *L. monocytogenes*. Results are representative of two experiments.



and then examined the cells for activation and apoptosis markers by flow cytometry. After treatment, wild-type monocytes had higher expression of major histocompatibility complex (MHC) class II (Fig. 7c, left), more secretion of nitric oxide (Fig. 7c, right) and a higher forward-scatter-side-scatter profile (Fig. 7d), which indicated that they had become activated and differentiated. The percentage of wild-type annexin V-positive cells also decreased after treatment (Fig. 7e). In contrast, most *elektra*-homozygous monocytes failed to upregulate MHC class II (Fig. 7c, left), and nitric oxide could not be detected in the culture medium (Fig. 7c, right). The percentage of annexin V-positive *elektra*-homozygous monocytes increased, and indeed most seemed to be dead, as indicated by their low forward-scatter-side-scatter profile (Fig. 7d,e). These results demonstrate that similar to *elektra*-homozygous T cells, monocytes also undergo apoptosis in response to activation.

A mutation in *Slfn2* produces the *elektra* phenotype

We mapped the mutation responsible for the *elektra* phenotype to chromosome 11 by assessing CD8⁺ T cell deficiency in the blood (Supplementary Fig. 6a,b) and then further confined this to a critical region 5.5 megabases in size bounded by the markers D11Mit34 and D11Mit119 (located 79 and 83.5 megabases from the centromere, respectively; Supplementary Fig. 6c). The critical region contained a total of 116 annotated candidate genes (Supplementary Fig. 6d). We targeted all coding exons in the region for automated sequencing, and 69.7% high-quality coverage of mutant and control templates was achieved on first pass. We identified a single point mutation in the region in *Slfn2* (Supplementary Fig. 6e), which encodes one member of a paralogous family of proteins with largely unknown function. The mutation resulted in an isoleucine-to-asparagine substitution of residue 135 of the encoded 278-amino acid protein (Supplementary Fig. 6f). We used bacterial artificial chromosome (BAC) transgenesis to restore the *elektra* CD8⁺ T cell phenotype (Fig. 8a,b), thus confirming the causative relationship between the mutation and the observed phenotype. We infer that *elektra* is a loss-of-function rather than a gain-of-function allele, first because the phenotype is recessive and second because transgenesis with the wild-type sequence restored the phenotype instead of worsening it. The listeria susceptibility and MCMV susceptibility were also abolished by transgene 'rescue' (Fig. 8c,d).

In addition to studying mice homozygous for the *elektra* mutation (*Slfn2*^{eka/eka}), we generated *Slfn1*^{-/-} and *Slfn3*^{-/-} mice by gene targeting and examined their phenotypes. Consistent with a published report²⁹, *Slfn1*^{-/-} mice did not have a lower number or frequency of

T cells, NK cells, monocytes or CD19⁺ B cells in the blood, spleen or thymus (Supplementary Fig. 7a and data not shown). *Slfn3*^{-/-} mice also showed no evident altered immune phenotype (Supplementary Fig. 7b). We conclude that *Slfn2* has a nonredundant function in regulating the survival of peripheral T cells and inflammatory monocytes, whereas *Slfn1* and *Slfn3* do not.

DISCUSSION

Our results have demonstrated that a mutation in *Slfn2* caused immunodeficiency as a consequence of T cell and monocyte apoptosis secondary to a semiactivated phenotype. Many of our findings suggested that this semiactivated state in *Slfn2*^{eka/eka} T cells stemmed from a loss of cellular quiescence. First, *Slfn2*^{eka/eka} T cells had a higher percentage of cells replicating DNA both in the steady state and during the initial response to TCR stimulation, suggestive of a greater readiness to enter S phase. Second, unstimulated *Slfn2*^{eka/eka} T cells had a unique phenotype in which naive (CD44^{lo}) T cells had low expression of CD62L and IL-7R α , and mature (CD44^{hi}) T cells had no expression of CD62L, IL-7R α or CD5 but had normal expression of CD69, indicative of a semiactivated phenotype.

The activation of several pathways, including the NF- κ B, NFAT, Akt, Erk1/2, Jnk and p38 pathways, regulates T cell survival. In *Slfn2*^{eka/eka} mice, we presume that as a result of a loss of quiescence, the balance among these pathways is altered to favor apoptosis rather than expansion. Indeed, we observed that p38 and Jnk were constitutively activated in unstimulated *Slfn2*^{eka/eka} T cells. Activation of these kinases is associated with T cell apoptosis^{15,16} and may represent a factor contributing to the apoptosis of *Slfn2*^{eka/eka} T cells. The enhancement of p38 and Jnk phosphorylation observed after TCR stimulation of *Slfn2*^{eka/eka} T cells and the fact that inflammatory monocytes (of the myeloid lineage) also undergo apoptosis after activation together suggest that the proliferative signals negatively regulated by *Slfn2* may be distinct from the TCR signaling pathways that lead to the development of activated T cell effector functions and full T cell activation.

Several studies have suggested that lymphocytes must actively maintain a quiescent state to remain resistant to apoptosis. IL-15 has

been shown to exert quiescence-inducing effects that are important for its antiapoptotic properties³⁰. Transcription factors that include members of the Foxo family⁶ and LKLF^{7,31} have also been shown to promote quiescence, and loss of their activity leads to induction of apoptosis. However, several studies have challenged the idea that Foxo and LKLF regulate the quiescent state itself, presenting evidence that these proteins instead control the expression of proteins associated with homing and survival^{32–34}. These reports suggest that impaired trafficking and survival of T cells creates a lymphopenic environment that leads to the loss of quiescence in peripheral T cells and raise the question of whether *Slfn2* actually controls survival or quiescence of T cells. *Slfn2*^{eka/eka} T cells were rescued from death by expression of a human antiapoptotic *BCL2* transgene. However, although T cells in these mice were not subject to a lymphopenic environment, they still had the same semiactivated phenotype as that of T cells from *Slfn2*^{eka/eka} mice. Similarly, in mixed-bone marrow chimeras, *Slfn2*^{eka/eka} T cells underwent apoptosis and had a semiactivated phenotype despite being in a normal, nonlymphopenic environment. Thus, our results indicate that the failure of mature *Slfn2*^{eka/eka} T cells to engage the antiapoptotic machinery of the cell stemmed from loss of quiescence and acquisition of a semiactivated phenotype by naive *Slfn2*^{eka/eka} T cells and was not a consequence of impaired survival signaling or activation by a lymphopenic environment. IL-7 and IL-15 are critical T cell growth and survival factors, and the absence of their signaling due to loss of expression of IL-7R α and IL-2R β in CD44^{hi} T cells may be the trigger that activates the intrinsic apoptotic pathway in *Slfn2*^{eka/eka} T cells.

Slfn2 is one of nine members of the *Slfn* gene family located in a cluster on mouse chromosome 11 (refs. 29,35). A tenth *Slfn* family member, *Slfn1*, is encoded by a gene on chromosome 4 (ref. 36). Although *Slfn2* has no human ortholog, it is most similar to *SLFN12* and *SLFN12L*, two of seven paralogs in the human genome. Aside from a divergent AAA (ATPase associated with various cellular activities) domain and a sequence designated COG2685 (National Center for Biotechnology Information conserved domain database) found in all *Slfn* proteins, *Slfn2* bears no similarity to other proteins^{29,35}. AAA domains, to which the divergent AAA domain is related, are present in proteins of the AAA family and mediate conformational and translocational changes of substrate proteins during cycles of nucleotide binding and hydrolysis^{37,38}. COG2685, a domain of unknown function, is predicted to contain a helix-turn-helix DNA-binding motif and bears similarity to a domain present in several ATP-dependent DNA helicases and transcriptional regulators³⁵. The *elektra* mutation, a T-to-A transversion, causes an isoleucine-to-asparagine substitution of residue 135 of the 278-amino acid *Slfn2* protein in a region in which no functional domains have been identified.

We hypothesize that *Slfn2* maintains the quiescent state by promoting the expression of quiescence genes and/or repression of genes required for proliferation or differentiation. Published work, mainly on the related *Slfn1* protein (53% identical), supports our hypothesis. Thymocyte-specific transgenic expression of *Slfn1* cDNA in mice results in a much smaller thymus due to impaired development of the CD4⁺CD8⁺ double-negative population in the thymus²⁹. *In vitro*, ectopic expression of *Slfn1* in fibroblasts represses cell growth and arrests cells in the G1 phase by causing transcriptional downregulation of cyclin D1 (refs. 29,35,39). Notably, *Slfn2* overexpression caused much stronger growth repression than does *Slfn1* overexpression⁹. The cyclin D genes are targets of Foxo transcription factors important in the regulation of quiescence⁶, which raises the possibility that the function of *Slfn2* intersects with the pathways controlling Foxo function.

We have shown that the *elektra* allele of *Slfn2* confers susceptibility to two very different viral infections (LCMV and MCMV) in mice. The susceptibility to LCMV is probably related to impairment of CD8⁺ T cell function. Notably, the mutation had no effect on NK cell numbers or function, although these cells are known to be essential for defense against MCMV. We consider it possible that inflammatory monocytes fulfill an essential function as well, given that lymphocytes are not needed for survival during the first several weeks after inoculation with MCMV¹⁰. Indeed, monocyte and macrophage cells are suggested to be protective in influenza infection⁴⁰, and inflammatory monocytes are essential for defense against *L. monocytogenes* infection²⁸. A nonredundant role has been directly demonstrated for inflammatory monocytes in controlling viral infection⁴¹.

Several orthopoxviruses contain either full-length or fragmentary *Slfn* homologs. The full-length camelpox v-SLFN is most similar to mouse *Slfn1* and *Slfn2*, with approximately 30% amino acid identity in the conserved region. A recombinant vaccinia virus strain expressing camelpox v-SLFN has been shown to be attenuated relative to the wild-type virus when mice are infected intranasally, resulting in less weight loss and more rapid recovery⁴². Viruses thus seem to have appropriated a *Slfn* sequence and may use it to manipulate the survival and proliferation of host cells of the immune response and, hence, the immunopathological consequences of infection.

METHODS

Methods and any associated references are available in the online version of the paper at <http://www.nature.com/natureimmunology/>.

Note: Supplementary information is available on the Nature Immunology website.

ACKNOWLEDGMENTS

We thank O. Milstein, J.F. Purton and K. Brandl for discussions; M.B.A. Oldstone (The Scripps Research Institute) for the Armstrong strain of LCMV; and C.D. Surh (The Scripps Research Institute) for monoclonal anti-IL-7 (M25). Supported by the European Molecular Biology Organization (M.B. and P.K.), the Swiss National Science Foundation (P.K.) and the US National Institutes of Health (PO1 AI070167-01).

AUTHOR CONTRIBUTIONS

M.B. and B.B. designed the research with critical suggestions from P.K., K.C. and A.N.T.; M.B., P.K., K.C., X.L., B.A.C., O.M.S., D.P. and B.R.L. did experiments; X.L. and X.D. generated the BAC-transgenic mice; M.B., Y.X. and K.K. did all genome mapping; T.S., O.T. and S.A. generated *Slfn3*^{-/-} and *Slfn1*^{-/-} mice; and M.B., E.M.Y.M. and B.B. wrote the manuscript.

COMPETING FINANCIAL INTERESTS

The authors declare no competing financial interests.

Published online at <http://www.nature.com/natureimmunology/>.

Reprints and permissions information is available online at <http://npg.nature.com/reprintsandpermissions/>.

1. Yusuf, I. & Fruman, D.A. Regulation of quiescence in lymphocytes. *Trends Immunol.* **24**, 380–386 (2003).
2. Chechlinska, M. *et al.* Molecular signature of cell cycle exit induced in human T lymphoblasts by IL-2 withdrawal. *BMC Genomics* **10**, 261 (2009).
3. Collier, H.A., Sang, L. & Roberts, J.M. A new description of cellular quiescence. *PLoS Biol.* **4**, e83 (2006).
4. Glynn, R., Ghandour, G., Rayner, J., Mack, D.H. & Goodnow, C.C. B-lymphocyte quiescence, tolerance and activation as viewed by global gene expression profiling on microarrays. *Immunol. Rev.* **176**, 216–246 (2000).
5. Teague, T.K. *et al.* Activation changes the spectrum but not the diversity of genes expressed by T cells. *Proc. Natl. Acad. Sci. USA* **96**, 12691–12696 (1999).
6. Tothova, Z. *et al.* FoxOs are critical mediators of hematopoietic stem cell resistance to physiologic oxidative stress. *Cell* **128**, 325–339 (2007).
7. Kuo, C.T., Veselits, M.L. & Leiden, J.M. LKLF: A transcriptional regulator of single-positive T cell quiescence and survival. *Science* **277**, 1986–1990 (1997).
8. Tzachanis, D. *et al.* Tob is a negative regulator of activation that is expressed in anergic and quiescent T cells. *Nat. Immunol.* **2**, 1174–1182 (2001).

9. Crozat, K. *et al.* Analysis of the MCMV resistome by ENU mutagenesis. *Mamm. Genome* **17**, 398–406 (2006).
10. Webb, J.R., Lee, S.H. & Vidal, S.M. Genetic control of innate immune responses against cytomegalovirus: MCMV meets its match 3. *Genes Immun.* **3**, 250–262 (2002).
11. Jiang, Z. *et al.* Details of Toll-like receptor:adapter interaction revealed by germ-line mutagenesis. *Proc. Natl. Acad. Sci. USA* **103**, 10961–10966 (2006).
12. Macian, F. NFAT proteins: key regulators of T-cell development and function. *Nat. Rev. Immunol.* **5**, 472–484 (2005).
13. Li, Q. & Verma, I.M. NF- κ B regulation in the immune system. *Nat. Rev. Immunol.* **2**, 725–734 (2002).
14. Juntilla, M.M. & Koretzky, G.A. Critical roles of the PI3K/Akt signaling pathway in T cell development. *Immunol. Lett.* **116**, 104–110 (2008).
15. Wada, T. & Penninger, J.M. Mitogen-activated protein kinases in apoptosis regulation. *Oncogene* **23**, 2838–2849 (2004).
16. Rincon, M. & Pedraza-Alva, G. JNK and p38 MAP kinases in CD4⁺ and CD8⁺ T cells. *Immunol. Rev.* **192**, 131–142 (2003).
17. Boyman, O., Ramsey, C., Kim, D.M., Sprent, J. & Surh, C.D. IL-7/anti-IL-7 mAb complexes restore T cell development and induce homeostatic T cell expansion without lymphopenia. *J. Immunol.* **180**, 7265–7275 (2008).
18. Kieper, W.C. & Jameson, S.C. Homeostatic expansion and phenotypic conversion of naive T cells in response to self peptide/MHC ligands. *Proc. Natl. Acad. Sci. USA* **96**, 13306–13311 (1999).
19. Goldrath, A.W., Bogatzki, L.Y. & Bevan, M.J. Naive T cells transiently acquire a memory-like phenotype during homeostasis-driven proliferation. *J. Exp. Med.* **192**, 557–564 (2000).
20. Cho, B.K., Rao, V.P., Ge, Q., Eisen, H.N. & Chen, J. Homeostasis-stimulated proliferation drives naive T cells to differentiate directly into memory T cells. *J. Exp. Med.* **192**, 549–556 (2000).
21. Khaled, A.R. & Durum, S.K. Lymphocyte: cytokines and the control of lymphoid homeostasis. *Nat. Rev. Immunol.* **2**, 817–830 (2002).
22. Hildeman, D.A. *et al.* Activated T cell death *in vivo* mediated by proapoptotic bcl-2 family member bim. *Immunity* **16**, 759–767 (2002).
23. Pellegrini, M., Belz, G., Bouillet, P. & Strasser, A. Shutdown of an acute T cell immune response to viral infection is mediated by the proapoptotic Bcl-2 homology 3-only protein Bim. *Proc. Natl. Acad. Sci. USA* **100**, 14175–14180 (2003).
24. Krammer, P.H., Arnold, R. & Lavrik, I.N. Life and death in peripheral T cells. *Nat. Rev. Immunol.* **7**, 532–542 (2007).
25. Boyman, O., Cho, J.H., Tan, J.T., Surh, C.D. & Sprent, J. A major histocompatibility complex I-dependent subset of memory phenotype CD8⁺ cells. *J. Exp. Med.* **203**, 1817–1825 (2006).
26. Oehen, S. & Brduscha-Riem, K. Differentiation of naive CTL to effector and memory CTL: correlation of effector function with phenotype and cell division. *J. Immunol.* **161**, 5338–5346 (1998).
27. Chao, C.C., Jensen, R. & Dailey, M.O. Mechanisms of L-selectin regulation by activated T cells. *J. Immunol.* **159**, 1686–1694 (1997).
28. Serbina, N.V. *et al.* Sequential MyD88-independent and -dependent activation of innate immune responses to intracellular bacterial infection. *Immunity* **19**, 891–901 (2003).
29. Schwarz, D.A., Katayama, C.D. & Hedrick, S.M. Schlafen, a new family of growth regulatory genes that affect thymocyte development. *Immunity* **9**, 657–668 (1998).
30. Dooks, H. *et al.* Quiescence-inducing and antiapoptotic activities of IL-15 enhance secondary CD4⁺ T cell responsiveness to antigen. *J. Immunol.* **161**, 2141–2150 (1998).
31. Buckley, A.F., Kuo, C.T. & Leiden, J.M. Transcription factor LKLF is sufficient to program T cell quiescence via a c-Myc-dependent pathway. *Nat. Immunol.* **2**, 698–704 (2001).
32. Bai, A., Hu, H., Yeung, M. & Chen, J. Kruppel-like factor 2 controls T cell trafficking by activating L-selectin (CD62L) and sphingosine-1-phosphate receptor 1 transcription. *J. Immunol.* **178**, 7632–7639 (2007).
33. Carlson, C.M. *et al.* Kruppel-like factor 2 regulates thymocyte and T-cell migration. *Nature* **442**, 299–302 (2006).
34. Kerdales, Y.M. *et al.* Foxo1 links homing and survival of naive T cells by regulating L-selectin, CCR7 and interleukin 7 receptor. *Nat. Immunol.* **10**, 176–184 (2009).
35. Geserick, P., Kaiser, F., Klemm, U., Kaufmann, S.H. & Zerrahn, J. Modulation of T cell development and activation by novel members of the Schlafen (slfn) gene family harbouring an RNA helicase-like motif. *Int. Immunol.* **16**, 1535–1548 (2004).
36. Ferguson, D.A., Chiang, J.T., Richardson, J.A. & Graff, J. eXPRESSION: an in silico tool to predict patterns of gene expression. *Gene Expr. Patterns* **5**, 619–628 (2005).
37. Hanson, P.I. & Whiteheart, S.W. AAA+ proteins: have engine, will work. *Nat. Rev. Mol. Cell Biol.* **6**, 519–529 (2005).
38. White, S.R. & Lauring, B. AAA+ ATPases: achieving diversity of function with conserved machinery. *Traffic* **8**, 1657–1667 (2007).
39. Brady, G., Boggan, L., Bowie, A. & O'Neill, L.A. Schlafen-1 causes a cell cycle arrest by inhibiting induction of cyclin D1. *J. Biol. Chem.* **280**, 30723–30734 (2005).
40. Kaufmann, A. *et al.* Defense against influenza A virus infection: essential role of the chemokine system. *Immunobiology* **204**, 603–613 (2001).
41. Barbalat, R., Lau, L., Locksley, R.M. & Barton, G.M. Toll-like receptor 2 on inflammatory monocytes induces type I interferon in response to viral but not bacterial ligands. *Nat. Immunol.* **10**, 1200–1207 (2009).
42. Gubser, C. *et al.* Camelpox virus encodes a schlafen-like protein that affects orthopoxvirus virulence. *J. Gen. Virol.* **88**, 1667–1676 (2007).

ONLINE METHODS

Mice and MCMV-susceptibility screen. C57BL/6J (wild-type) mice, C3H/HeN mice, C57BL/6 *Cd3e*^{m1B^{tr}} mice and C57BL/6 *Myd88*^{Poc} mice were maintained in specific pathogen-free conditions in the vivarium of The Scripps Research Institute, and all studies involving mice were done in accordance with institutional regulations governing animal care and use. C57BL/6J mice, which are naturally resistant to MCMV, were used for mutagenesis as described⁴³. The conditions of the *in vivo* MCMV-susceptibility screen have been described⁹. B6.Cg-Tg(BCL2)25Wehi/J mice, B6.MRL-*Fas*^{l^{pr}/J} mice and C57BL/6.SJL (*Ptprc*^{aPep3^b}; Ly5.1⁺) were from The Jackson Laboratory. The elektra strain is described on the Mutagenetix website and may be obtained from the Mutant Mouse Regional Resource Center.

Infection with MCMV, LCMV and *L. monocytogenes*. Preparation of the MCMV stock (Smith strain) has been described⁹. Mice were infected with MCMV by intraperitoneal injection. The Armstrong strain of LCMV (provided by M.B.A. Oldstone) was injected intravenously. Viral loads were determined after organ homogenization in DMEM plus 3% (vol/vol) FCS by standard plaque assay on NIH3T3 fibroblast cells (for MCMV) and on Vero monkey kidney cells (for LCMV). For *in vivo* challenge with *L. monocytogenes* (strain 10403S; Xenogen), bioluminescent bacteria were prepared and then injected intravenously as described⁴⁴.

Genetic mapping. Because most inbred strains show either a strong or moderate susceptibility to MCMV infection, the chromosome location of the *elektra* mutation was mapped using the phenotype of low frequency of CD8⁺ T cells. Initial confinement of the mutation was made by outcrossing of *Slfn2*^{eka/eka} mice to C3H/HeN mice, followed by backcrossing of F₁ hybrids to the *Slfn2*^{eka/eka} stock. The frequency of CD8⁺ T cells in the blood of 6-week-old F₂ mice was analyzed by flow cytometry. Linkage was measured by comparison with a panel of 129 markers distributed across the genome at 50-megabase intervals. Additional microsatellite markers were used in fine-mapping studies.

Transgenesis. The BAC clone RP23-246H3, which represents a 197-kilobase genomic DNA fragment between positions 82798126 and 82995557 on chromosome 11, was obtained from Children's Hospital Oakland Research Institute and was microinjected into the male pronucleus of >100 fertilized *Slfn2*^{eka/eka} oocytes to produce transgenic mice. Embryos were transferred to pseudopregnant CD1 female mice and a total of twelve pups were born. Among those, seven mice were confirmed as transgenic founders by sequencing of DNA amplified across the *Slfn2*^{eka} mutation site. In the five remaining mice, only the mutant *Slfn2* sequence was present.

***In vivo* assay for NK cell cytotoxicity.** The *in vivo* assay for NK cell cytotoxicity was done as described⁴⁵.

Isolation of NK cells, CD8⁺ T cells and monocytes. NK cells, CD8⁺ T cells or dendritic cells were isolated from spleens with the antibody DX5 (anti-CD49b; 130-052-501), a CD8⁺ T cell isolation kit (130-090-859) or a CD11c MACS cell-separation kit (130-052-001), respectively, according to the manufacturer's instructions (Miltenyi Biotec).

For monocyte purification, bone marrow cells were stained with allophycocyanin-conjugated anti-CD11b (M1/70; eBioscience), fluorescein isothiocyanate-conjugated anti-Ly6C (AL-21; BD Biosciences) and phycoerythrin-conjugated anti-Ly6G (1A8; Biolegend). Then the CD11b⁺, Ly6C^{hi} and Ly6G⁻ subpopulations were sorted with a FACSAria (BD).

***Ex vivo* restimulation of CD8⁺ cells.** Splenocytes from LCMV-infected mice were restimulated for 4 h with various concentrations of the LCMV peptides gp33 or NP396 in the presence of brefeldin A (BD Biosciences), after which IFN- γ production was measured by intracellular staining.

***In vitro* T cell proliferation assay and BrdU-incorporation assay.** Lymph node or spleen cells were labeled for 10 min with CFSE (carboxyfluorescein diacetate succinimidyl ester), followed by two washing steps. Cells were plated in 24-well plates coated with anti-CD3 ϵ (10 μ g/ml; 145-2C11; eBioscience) and anti-CD28 (10 μ g/ml; 37.51; eBioscience) or were plated in uncoated

24-well plates and then were treated with mouse IL-2 (100 ng/ml; eBioscience) or phorbol 12-myristate 13-acetate plus ionomycin. Cells were collected at various time points and CFSE intensity was analyzed by flow cytometry.

For BrdU incorporation, after activation of cells, BrdU (BD Biosciences) was added for 90 min. Cells were stained with anti-BrdU (3D4; BD Biosciences), followed by flow cytometry.

Adoptive transfer of T cells, thymectomy and bone marrow transplantation. For adoptive transfer, CFSE-labeled spleen cells were injected intravenously into recipient mice that had been sublethally irradiated (600 rads) 24 h earlier. At 7 d after adoptive transfer, splenocytes were prepared, their surfaces were stained for CD45.1 (A20; eBioscience) together with CD8 (53-6.7; eBioscience) or CD4 (L3T4, eBioscience) and then they were analyzed by flow cytometry for CFSE dilution.

Thymuses were removed by suction from 7-week-old male mice anesthetized with ketamine (100 mg per kg body weight) and xylazine (10 mg per kg body weight)⁴⁶. Mice with incomplete removal of the thymus were excluded from analysis.

For bone marrow transplantation, bone marrow cells were extracted from femurs and tibias and were placed in a solution of 0.1% (vol/vol) BSA in PBS. Bone marrow cells (5×10^6) were injected intravenously into the lateral tail veins of recipient mice that had been irradiated (1,000 rads) 24 h earlier. For mixed-bone marrow chimeras, equal numbers of bone marrow cells from congenic wild-type (C57BL/6.SJL; *Ptprc*^{aPep3^b}; Ly5.1⁺) mice and *Slfn2*^{eka/eka} (Ly5.2⁺) mice were injected into irradiated (1,000 rads) CD3-deficient mice.

Injection of IL-7 plus anti-IL-7 *in vivo*. Recombinant IL-7 (1.5 μ g) and monoclonal anti-IL-7 (7.5 μ g; M25; a gift from C.D. Surh) were preincubated together for 10 min at 25 °C, then PBS was added up to a volume of 0.4 ml. Mice were injected intraperitoneally once or twice at 3-d intervals with IL-7-anti-IL-7 complexes or PBS.

Nitric oxide measurement. Nitrite concentrations were measured by the Griess reaction.

Antibodies. The following antibodies were used for flow cytometry: anti-CD8 α (53-6.7), anti-CD4 (L3T4), anti-CD3 ϵ (145-2C11), anti-CD5 (J3-7.3), anti-CD25 (PC61.5), anti-CD45.1(A20), anti-CD45.2 (104), anti-CD69 (H1.2F3), anti-IFN- γ (XMG1.2), anti-Bcl-2 (10C4), anti-CD44 (IM7), anti-CD122 (TM-b1), anti-Qa-2 (1-1-2), anti-Fas (15A7), anti-CD11b (M1/70), anti-TCR β (H57-597), anti-B220 (RA3-6B2) and anti-NK1.1 (PK 136; all from eBioscience); anti-Ly6G (1A8; Biolegend); antibody to Jnk phosphorylated at Thr183 and Tyr185 (9251), antibody to p38 phosphorylated at Thr180 and Tyr182 (9211), and antibody to Akt phosphorylated at Ser473 (193H12) or Thr308 (9275; all from Cell Signaling Technology); and anti-Ly6C (AL-21; BD Biosciences). The following antibodies were used for immunoblot analysis: antibody to p38 phosphorylated Thr180 and Tyr182 (9211), anti-p38 (9212), antibody to phosphorylated Erk1/2 (9101) and anti-p65 (3034; all from Cell Signaling Technology); and anti-NFAT1 (MA1-025; Affinity Bioreagents). Purified anti-CD3 ϵ (145-2C11) and anti-CD28 (37.51; both from eBioscience) were used at the appropriate concentration for T cell activation. Annexin V (BD Biosciences) was used for the identification of proapoptotic T cells.

Statistical analysis. The statistical significance of differences was determined by the two-tailed Student's *t*-test. Differences with a *P* value of less than 0.05 were considered statistically significant.

43. Hoebe, K., Du, X., Goode, J., Mann, N. & Beutler, B. *Lps2*: a new locus required for responses to lipopolysaccharide, revealed by germline mutagenesis and phenotypic screening. *J. Endotoxin Res.* **9**, 250-255 (2003).

44. Rutschmann, S. *et al.* PanR1, a dominant negative missense allele of the gene encoding TNF- α (Tnf), does not impair lymphoid development. *J. Immunol.* **176**, 7525-7532 (2006).

45. Krebs, P. *et al.* NK-cell-mediated killing of target cells triggers robust antigen-specific T-cell-mediated and humoral responses. *Blood* **113**, 6593-6602 (2009).

46. Reeves, J.P., Reeves, P.A. and Chin, L.T. in *Current Protocols in Immunology* (eds. Coligan, J.E. *et al.*) 1.10.5-1.10.6 (John Wiley & Sons, Hoboken, New Jersey, 2009).